A study of possible extra-framework cation ordering in *Pbca* leucite structures with stoichiometry $RbCsX^{2+}Si_5O_{12}$ (X = Mg, Ni, Cd)

Anthony M. T. Bell [1,a] and C. Michael B. Henderson[2]
[1]*Materials and Engineering Research Institute, Sheffield Hallam University, Sheffield, S1 1WB, UK*
[2]*School of Earth and Environmental Sciences, University of Manchester, Manchester, M13 9PL, UK*

(Received 13 September 2018; accepted 27 December 2018)

Leucites are silicate framework structures with some of the silicon framework cations partially replaced by divalent or trivalent cations. A monovalent extraframework alkali metal cation is also incorporated to balance the charges. We have previously reported *Pbca* leucite structures with the stoichiometries $Cs_2X^{2+}Si_5O_{12}$ (X = Mg, Mn, Co, Ni, Cu, Zn, Cd) and $Rb_2X^{2+}Si_5O_{12}$ (X = Mg, Mn, Ni, Cd). These orthorhombic leucite structures have all the silicon and non-silicon framework cations completely ordered onto separate crystallographic sites. This structure has five distinct Si sites and 1 X site; there are also two distinct sites for the extra-framework Cs or Rb. We have recently synthesised leucite analogues with two different extra-framework cations, these have the stoichiometry $RbCsX^{2+}Si_5O_{12}$ (X = Mg, Ni, Cd). The initial Rietveld refinements assumed 50% Cs and 50% Rb on each of the two extra-framework cation sites. The refined structures for X = Ni and Cd have (within error limits) complete extra-framework cation site disorder. However, for X = Mg there is partial ordering of the extra-framework cation sites, the site occupancies are:- Cs1 0.37(3), Rb1 0.63(3), Cs2 0.63(3), Rb2 0.37(3). © *2019 International Centre for Diffraction Data.*
[doi:10.1017/S0885715619000071]

Key words: X-ray powder diffraction, Rietveld refinement, silicate framework minerals

I. INTRODUCTION

Synthetic anhydrous analogues of the silicate framework minerals leucite ($KAlSi_2O_6$) and pollucite ($CsAlSi_2O_6$) can be prepared with the general formulae $A_2BSi_5O_{12}$ and $ACSi_2O_6$; where A is a monovalent alkali metal cation, B is a divalent cation and C is a trivalent cation. These structures all have the same topology with B and C cations partially substituting onto tetrahedrally coordinated sites (T-sites) in the silicate framework and charge balancing A cations sitting in extra-framework channels. The A cations can be replaced by ion exchange, Cs containing silicate framework minerals are of potential technological interest as storage media for radioactive Cs from nuclear waste (Gatta *et al*., 2008).

We have used X-ray and neutron powder diffraction to determine and Rietveld refine the ambient temperature crystal structures of leucite analogues with the general formulae $A_2BSi_5O_{12}$ and $ACSi_2O_6$. Crystal structures have been refined in the $Ia\bar{3}d$ cubic and $I4_1/a$ tetragonal space groups (A = K, Rb, Cs; B = Mg, Mn, Co, Cu, Zn; $C = Fe^{3+}$; Bell *et al*., 1994a, 2010; Bell and Henderson, 1994a,b, 2018). These structures all have disordered T-site cations and also have A cation sites fully occupied with either K, Rb or Cs. Crystal structures have also been refined at ambient temperature for $P2_1/c$ monoclinic crystal structures of leucite analogues with the general formulae $A_2BSi_5O_{12}$ (A = K, B = Mg, Fe^{2+}, Co, Zn; Bell *et al*., 1994a; Bell and Henderson, 2018) and also for *Pbca* orthorhombic (A = Rb; B = Mg, Mn, Ni, Cd; Bell and Henderson, 1996, 2009, 2016) and (A = Cs; B = Mg, Mn, Co, Ni, Cu, Zn, Cd; Bell *et al*., 1994b, 2010; Bell and Henderson, 1996, 2009) These structures all have ordered T-site cations and also have A cation sites fully occupied with either K, Rb or Cs. $Cs_2ZnSi_5O_{12}$ undergoes a reversible phase transition from *Pbca* to *Pa-3* on heating to 566 K (Bell and Henderson, 2012). $K_2MgSi_5O_{12}$ undergoes a phase transition from $P2_1/c$ to *Pbca* on heating to 622 K (Redfern and Henderson, 1996).

In this paper, we report the Rietveld (Rietveld, 1969) refinements of the *Pbca* crystal structures of three more tectosilicate, cation-ordered leucite analogues with both Rb and Cs on the A cation sites; these have the stoichiometry of $RbCsX^{2+}Si_5O_{12}$ (X = Mg, Ni, Cd). The *Pbca* structure has two different sites for A cations, this study is to discover whether these sites have Rb and Cs cation order?

II. EXPERIMENTAL

A. sample synthesis

$Rb_2X^{2+}Si_5O_{12}$ and $Cs_2X^{2+}Si_5O_{12}$ were prepared from appropriate stoichiometric mixtures of Rb_2CO_3, Cs_2CO_3, SiO_2, and XO (X = Mg, Ni, Cd; Bell *et al*., 1994b; Bell and Henderson, 1996, 2009, 2016) and then 50:50 mixtures of the Rb and Cs samples were made for each of the three pairs of samples with the same X^{2+} cation. For X = Ni the starting materials were both glasses, the mixture was sealed in a gold capsule and heated in a furnace at 1173 K for 7 days. For X = Cd and Mg the starting materials were both crystalline, the mixtures were sealed in a gold capsule (X = Cd) or a Pd-Ag alloy capsule (X = Mg) and these were heated in a furnace at 1173 K for 6 h.

[a]Author to whom correspondence should be addressed. Electronic mail: Anthony.Bell@shu.ac.uk

TABLE I. Refined lattice parameters and A site occupancies.

Cations		Lattice parameters			
A^+	X^{2+}	a(Å)	b(Å)	c(Å)	V(Å^3)
Rb	Mg	13.422(1)	13.406(1)	13.730(1)	2470.5(4)
Rb Cs	Mg	13.5676(9)	13.7115(1)	13.5366(9)	2518.2(3)
Cs	Mg	13.6371(5)	13.6689(1)	13.7280(5)	2559.0(2)
Rb	Ni	13.469(3)	13.480(3)	13.442(2)	2440.6(8)
Rb Cs	Ni	13.5399(5)	13.563(1)	13.560(1)	2490.1(3)
Cs	Ni	13.6147(3)	13.6568(5)	13.6583(5)	2539.5(1)
Rb	Cd	13.4121(1)	13.6816(1)	13.8558(1)	2542.53(5)
Rb Cs	Cd	13.6935(3)	13.8030(3)	13.8592(4)	2619.6(1)
Cs	Cd	13.6714(1)	13.8240(1)	13.8939(1)	2625.86(6)
Cations		A site cation occupancies			
A^+	X^{2+}	A1 Rb	A1 Cs	A2 Rb	A2 Cs
Rb	Mg	1	0	1	0
Rb Cs	Mg	0.63(3)	0.37(3)	0.37(3)	0.63(3)
Cs	Mg	0	1	0	1
Rb	Ni	1	0	1	0
Rb Cs	Ni	0.49(6)	0.51(6)	0.51(6)	0.49(6)
Cs	Ni	0	1	0	1
Rb	Cd	1	0	1	0
Rb Cs	Cd	0.52(2)	0.48(2)	0.48(2)	0.52(2)
Cs	Cd	0	1	0	1

B. X-ray powder diffraction data collection

After heating the samples were removed from the metal capsules, ground with a mortar and pestle and then mounted on low-background silicon wafers with a drop of acetone prior to ambient temperature X-ray powder diffraction. Data were collected for the X = Mg and Cd samples with a PANalytical X'Pert Pro MPD using Cu$K\alpha$ X-rays, a graphite monochromator and a 2.122°2θ wide 100 channel X'Celerator area detector. For X = Mg data were collected in eight scans lasting 61 h in total which were summed together. These data were collected over the range 10°–100°2θ with a step width of 0.0167°2θ and an effective counting time of 5150 s per point. The beam size was defined with a 20 mm mask, fixed antiscatter (¼°) and divergence (⅛°) slits. For X = Cd data were collected in eight scans lasting 64 h in total which were summed together. These data were collected over the range 10°–100°2θ with a step width of 0.0167°2θ and an effective counting time of 5570 s per point. The beam size was defined with a 15 mm mask, fixed antiscatter (¼°) and divergence (⅛°) slits. For the X = Ni sample data were collected with a PANalytical Empyrean diffractometer using Co $K\alpha$ X-rays with an iron β-filter and a 3.3473°2θ wide 255 channel PIXCEL-3D area detector. Data were collected in two scans over 28 h. These data were collected over the range 15°–100°2θ with a step width of 0.0131°2θ and an effective counting time of 2487 s per point, the beam size was defined with a 20 mm mask, fixed divergence antiscatter (¼°) slit and automatic divergence slit with a 20 mm long beam footprint. These diffracted intensities for the X = Ni sample were summed and then converted from automatic divergence slit mode to fixed divergence slit mode in High Score Plus (PANalytical, 2009) prior to data analysis. No smoothing or α_2 stripping was done on any of these data. Both diffractometers were calibrated with an external NIST 640e silicon standard.

C. X-ray powder diffraction data analysis

Analyses of the summed powder diffraction data for each sample showed that all samples were single-phase and isostructural with the *Pbca* structure of $Cs_2CdSi_5O_{12}$ (Bell *et al.*, 1994b). Rietveld refinements were done using FULLPROF (Rodríguez-Carvajal, 1993), using the structures of $Rb_2XSi_5O_{12}$ (Bell and Henderson, 1996, 2009, 2016) as starting models but with half the Rb replaced by Cs. Backgrounds were fitted by linear interpolation between a set of background points with refinable heights. The Thompson-Cox-Hastings Pseudo-Voigt function (van Laar and Yelon, 1984), convoluted with asymmetry because of axial divergence (Finger *et al.*, 1994), was used to model the profile shape. For X = Mg data over the range 10°–71.5°2θ were

TABLE II. Refined interatomic distances and angles.

Cations		Interatomic distances			
A^+	X^{2+}	*A*1-O(Å)	*A*2-O(Å)	*X*-O(Å)	mean Si-O(Å)
Rb	Mg	3.48(3)	3.50(3)	1.90(3)	1.62(4)
Rb Cs	Mg	3.45(5)	3.62(5)	1.90(3)	1.61(2)
Cs	Mg	3.51(4)	3.57(5)	1.87(5)	1.61(5)
Rb	Ni	3.37(6)	3.51(6)	1.90(2)	1.64(2)
Rb Cs	Ni	3.48(9)	3.5(1)	1.89(5)	1.61(5)
Cs	Ni	3.42(5)	3.5(1)	1.88(4)	1.63(5)
Rb	Cd	3.41(2)	3.45(2)	2.22(1)	1.61(2)
Rb Cs	Cd	3.50(3)	3.55(2)	2.24(2)	1.61(2)
Cs	Cd	3.47(2)	3.53(2)	2.24(2)	1.59(2)
Cations		Interatomic angles (°)			
A^+	X^{2+}	Mean Si-O-Si	Mean Si-O-*X*	Mean O-Si-O	Mean O-*X*-O
Rb	Mg	141(2)	144(2)	108(2)	113(1)
Rb Cs	Mg	144(1)	145(1)	109(3)	109(3)
Cs	Mg	146(1)	143(1)	109(3)	109(2)
Rb	Ni	143(2)	125(2)	108(4)	109(3)
Rb Cs	Ni	145(3)	135(2)	108(6)	109(5)
Cs	Ni	142(3)	135(3)	109(3)	110(2)
Rb	Cd	142(1)	121.1(9)	109.4(9)	109.7(6)
Rb Cs	Cd	145(1)	122.9(8)	109(2)	109(1)
Cs	Cd	147(2)	127(1)	109(1)	109.5(7)

https://doi.org/10.1017/S0885715619000071 Published online by Cambridge University Press

TABLE III. Tetrahedral angle variance.

Cations		O-T-O variance (T = *X*, Si)	
A^+	X^{2+}	σ^2 (*X*) deg^2	mean σ^2 (Si) deg^2
Rb	Mg	107	246(172)
Rb Cs	Mg	43	147(51)
Cs	Mg	80	151(136)
Rb	Ni	44	309(112)
Rb Cs	Ni	42	262(133)
Cs	Ni	47	79(13)
Rb	Cd	163	26(13)
Rb Cs	Cd	59	134(25)
Cs	Cd	94	47(23)

Tetrahedral angle variance [σ^2, deg^2]: $\sigma^2 = \Sigma(\theta\text{-}109.47)^2/5$ (Robinson *et al.*, 1971) where θ is the O-T-O tetrahedral angle. Mean variance and standard deviation is given for the five Si tetrahedral sites in each structure.

used for data analysis as there were no visible Bragg reflections above 71.5°2θ. For *X* = Cd the whole 10°– 100°2θ range was used and for *X* = Ni the whole 15°–100°2θ range was used. Soft distance restraints were used on the Si-O and *X*-O distances. Si-O distances were restrained at 1.61 ± 0.01 Å; this distance is intermediate over the typical distance for tetrahedrally coordinated Si-O in framework silicates (1.59–1.63 Å; *International Tables for X-ray Crystallography*, 1985, Vol. III). Ni-O and Mg-O distances were restrained at 1.89 ± 0.01 Å; these distances are similar to those determined for *X* = Ni (Bell and Henderson, 1996, 2016), $K_2MgSi_5O_{12}$ (Bell *et al.*, 1994a) and $Cs_2MgSi_5O_{12}$ (Bell and Henderson, 2009) leucites. Cd-O distances were restrained at 2.23 ± 0.01 Å; these distances are similar to those determined for *X* = Cd (Bell *et al.*, 1994b; Bell and Henderson, 2009, 2012) leucites.

In these Rietveld refinements all atoms were located on the *Pbca* 8c Wyckoff general position. There are two distinct extraframework alkali metal cation sites for Rb and Cs. There are six T-sites, one for divalent X^{2+} cations and five for silicon cations, there are also twelve oxygen anion sites. Isotropic atomic displacement parameters were constrained to be the same for all sites occupied by silicon. Isotropic atomic displacement parameters were also constrained to be the same for all sites occupied by oxygen. As there is only one X^{2+} cation site then this site had no constraint on the isotropic atomic displacement parameter. Initial refinements had 50% Rb and 50% Cs on each of the two extraframework alkali metal cation sites, these site occupancies were allowed to refine but were constrained so that the sum of the occupancies for each element over the two sites was 100%. Isotropic atomic displacement parameters were constrained to be the same for Rb and Cs on the same alkali metal cation site but different to the isotropic atomic displacement parameters for Rb and Cs on the other alkali metal cation site. VESTA (Momma and Izumi, 2011) was used to plot crystal structures.

III. RESULTS AND DISCUSSION

Crystal structures have been refined for $RbCsX^{2+}Si_5O_{12}$ (*X* = Mg, Ni, Cd) leucite analogues from X-ray powder diffraction data. All are isostructural with their *Pbca* $Rb_2XSi_5O_{12}$ and $Cs_2XSi_5O_{12}$ analogues, with divalent *X* cations ordered onto separate T-sites than those occupied by Si. Table I shows the comparison of the refined lattice parameters and *A* cation site occupancies for $RbCsX^{2+}Si_5O_{12}$ compared to the published values for $Rb_2XSi_5O_{12}$ (Bell and Henderson, 1996, 2009, 2016) and $Cs_2XSi_5O_{12}$ (Bell and Henderson, 1996, 2009; Bell *et al.*, 1994b). Table II similarly shows refined interatomic distance and angles; the mean *X*-O and Si-O distances are close to the constraint distances, the mean O-*X*-O and O-Si-O angles are close to the ideal tetrahedral angle of 109.47°. Table III similarly shows the tetrahedral angle variances for the *X* and Si sites (Robinson *et al.*, 1971) in the silicate framework structures.

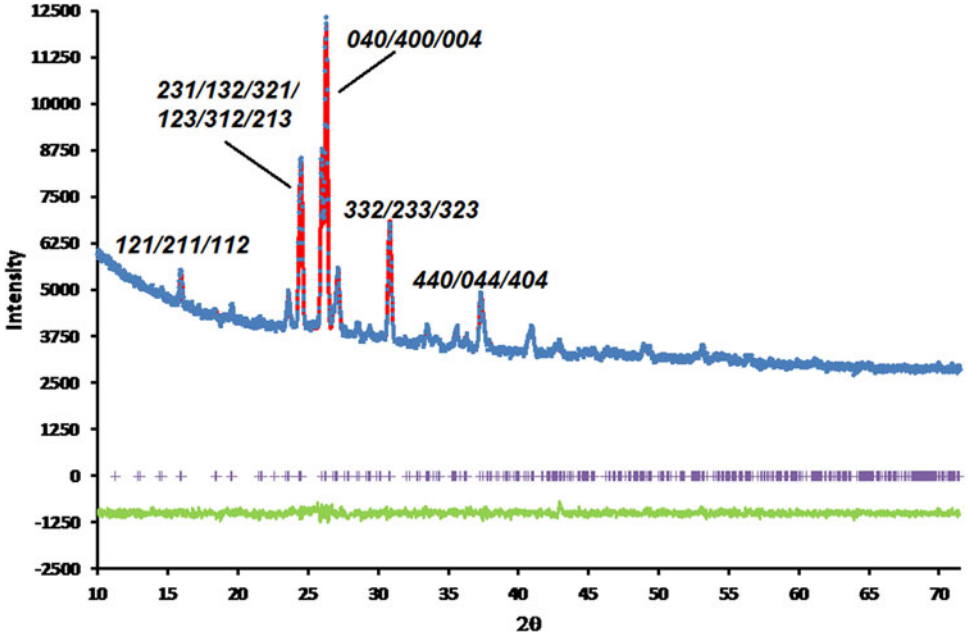

Figure 1. (color online) Rietveld difference plot for $RbCsMg^{2+}Si_5O_{12}$. Blue circles represent observed data points, red line represents calculated data points, green line represents difference curve and purple crosses represent positions of Bragg reflections. R-factors for this refinement were:- R_p = 1.2305, Rwp = 1.5794, R_{exp} = 1.6182, χ^2 = 0.9526. Miller indices are shown for some of the stronger peaks in the powder diffraction plot.

https://doi.org/10.1017/S0885715619000071 Published online by Cambridge University Press

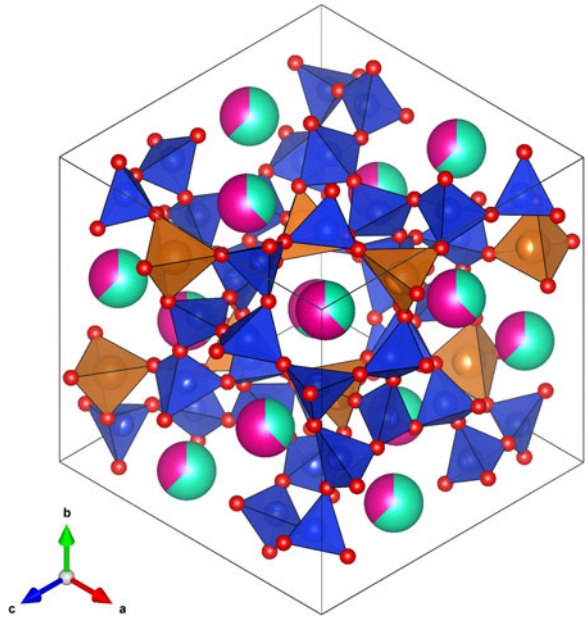

Figure 2. (color online) VESTA structure plot for $RbCsMg^{2+}Si_5O_{12}$, viewed down [111] showing a channel for extraframework Rb^+ and Cs^+ cations. SiO_4 tetrahedra are shown in blue, MgO_4 tetrahedra are shown in orange with O^{2-} anions are shown in red. Pink (Rb^+) and light blue (Cs^+) shadings show the occupancies of the two *A* cation sites.

A. $RbCsMg^{2+}Si_5O_{12}$ structure

Figures 1 and 2, respectively, show the Rietveld difference and the VESTA crystal structure plots for the refined crystal structure of $RbCsMg^{2+}Si_5O_{12}$, in Figure 2 light blue (Cs^+) and pink (Rb^+) shadings show the occupancies of the two *A* cation sites. Table I shows that this crystal structure has a unit cell volume which is approximately intermediate between those for $Rb_2Mg^{2+}Si_5O_{12}$ and $Cs_2Mg^{2+}Si_5O_{12}$. The refined occupancies of the two extraframework A sites are: Rb1 0.63(3), Cs1 0.37(3); Rb2 0.37(3), Cs2 0.63(3); there is some partial, but not complete, ordering of these occupancies. The greater occupancy of the larger Cs^+ cation on the extraframework *A*2 cation site is reflected in the larger *A*2-O distance compared to *A*1-O (see Table II). Table II also shows that the mean Si-O-Si and Si-O-*X* angles are similar for all *X* = Mg structures. Table III shows that the MgO_4 tetrahedron in the silicate framework structure for $RbCsMg^{2+}Si_5O_{12}$ is less distorted than those for $Rb_2Mg^{2+}Si_5O_{12}$ and $Cs_2Mg^{2+}Si_5O_{12}$.

B. $RbCsNi^{2+}Si_5O_{12}$ structure

Figures 3 and 4, respectively, show the Rietveld difference and the VESTA crystal structure plots for the refined crystal structure of $RbCsNi^{2+}Si_5O_{12}$, in Figure 4 light blue (Cs^+) and pink (Rb^+) shadings show the occupancies of the two *A* cation sites. Table I shows that this crystal structure also has a unit cell volume which is approximately intermediate between those for $Rb_2Ni^{2+}Si_5O_{12}$ and $Cs_2Ni^{2+}Si_5O_{12}$. The refined occupancies of the two extraframework A sites are: Rb1 0.49(6), Cs1 0.51(6); Rb2 0.51(6), Cs2 0.49(6). Within error limits there is complete disorder of these occupancies. For *X* = Ni the *A*-O distances for each of the two extraframework *A* cation sites are the same within error limits reflecting the disorder of Rb and Cs over these two sites. Table II also shows that the mean Si-O-Si angles are similar for all *X* = Ni structures but the corresponding Si-O-*X* angles are all smaller. The Si-O-*X* angle for $Rb_2Ni^{2+}Si_5O_{12}$ is smaller than those for $RbCsNi^{2+}Si_5O_{12}$ and $Cs_2Ni^{2+}Si_5O_{12}$. Table III shows that the NiO_4 tetrahedron in the silicate framework structure for $RbCsNi^{2+}Si_5O_{12}$ is slightly less distorted than those for $Rb_2Ni^{2+}Si_5O_{12}$ and $Cs_2Ni^{2+}Si_5O_{12}$.

C. $RbCsCd^{2+}Si_5O_{12}$ structure

Figures 5 and 6, respectively, show the Rietveld difference and the VESTA crystal structure plots for the refined crystal structure of $RbCsCd^{2+}Si_5O_{12}$, in Figure 6 light blue (Cs^+) and pink (Rb^+) shadings show the occupancies of the

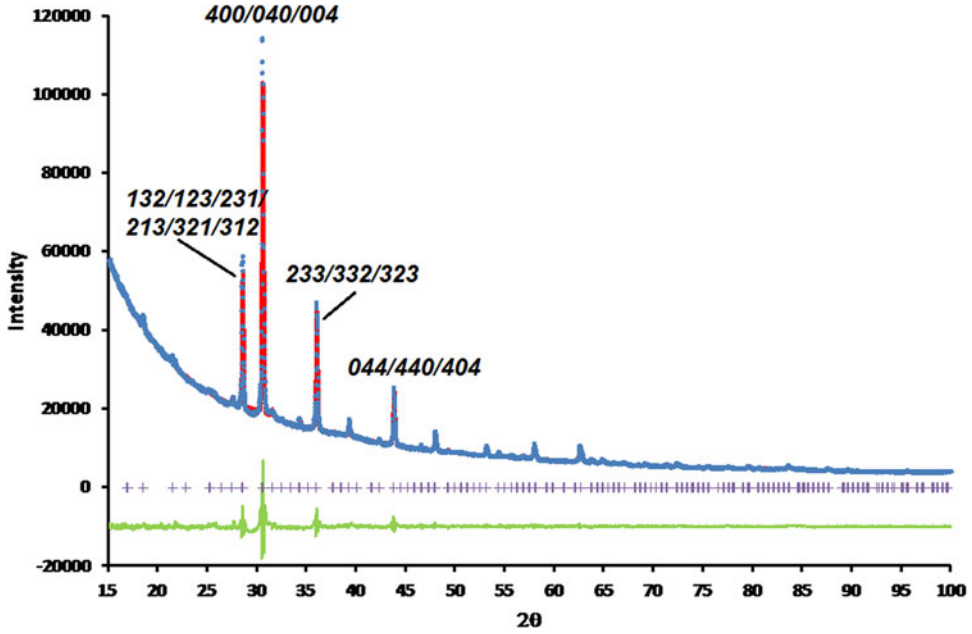

Figure 3. (Color online) Rietveld difference plot for $RbCsNi^{2+}Si_5O_{12}$. Blue circles represent observed data points, red line represents calculated data points, green line represents difference curve and purple crosses represent positions of Bragg reflections. R-factors for this refinement were:- $R_p = 1.6058$, Rwp = 2.7720, $R_{exp} = 0.8916$, $\chi^2 = 9.6659$. Miller indices are shown for some of the stronger peaks in the powder diffraction plot.

https://doi.org/10.1017/S0885715619000071 Published online by Cambridge University Press

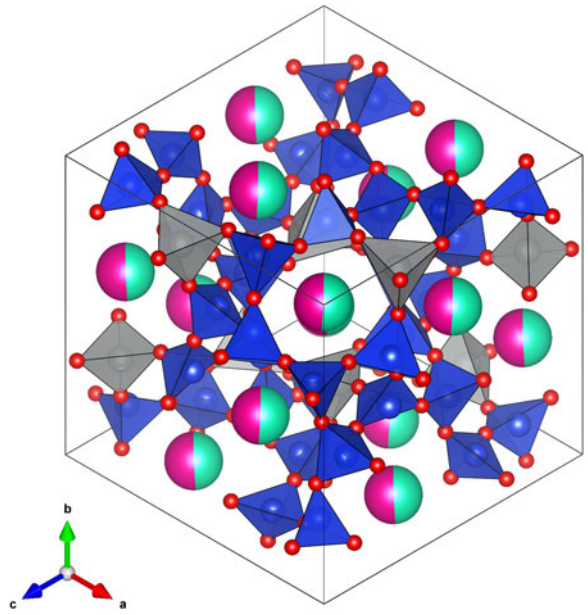

Figure 4. (color online) VESTA structure plot for $RbCsNi^{2+}Si_5O_{12}$, viewed down [111] showing a channel for extraframework Rb^+ and Cs^+ cations. SiO_4 tetrahedra are shown in blue, NiO_4 tetrahedra are shown in grey with O^{2-} anions are shown in red. Pink (Rb^+) and light blue (Cs^+) shadings show the occupancies of the two *A* cation sites.

two *A* cation sites. Table I shows that this crystal structure has a unit cell volume larger than that for $Rb_2Cd^{2+}Si_5O_{12}$ (Bell and Henderson, 1996) and smaller than that for $Cs_2Cd^{2+}Si_5O_{12}$ (Bell *et al*., 1994a,b). However, Table I shows that this crystal structure has a unit cell volume much closer to (but still smaller) than that for $Cs_2Cd^{2+}Si_5O_{12}$ than that for $Rb_2Cd^{2+}Si_5O_{12}$. The refined occupancies of the two extraframework A sites are: Rb1 0.52(2), Cs1 0.48(2); Rb2 0.48(2), Cs2 0.52(2). Within error limits there is complete disorder of these occupancies, similar to $RbCsNi^{2+}Si_5O_{12}$. For X = Cd the *A*-O distances for each of the two extraframework *A* cation sites are also the same within error limits reflecting the disorder of Rb and Cs over these two sites. Table III shows that the CdO_4 tetrahedra in the silicate framework structure for $RbCsCd^{2+}Si_5O_{12}$ is less distorted than those for $Rb_2Cd^{2+}Si_5O_{12}$ and $Cs_2Cd^{2+}Si_5O_{12}$. As was also seen for X = Ni, all X = Cd structures have larger mean Si-O-Si angles than the corresponding mean Si-O-*X* angles.

D. comparison of $RbCsX^{2+}Si_5O_{12}$ structures

The refined structure for X = Mg shows that having two different extraframework cation species results in structural changes compared to the structures with only one type extraframework cation. There are different mean *A*-O distances for the two *A* sites and partial *A* site cation ordering. For all X = Mg structures (with both one and two different extraframework cation species) the mean Si-O-Si and Si-O-*X* angles are similar.

However the refined structures for both X = Ni and Cd have similar mean *A*-O distances for the two *A* sites and no *A* site cation ordering. For all X = Ni and Cd structures (with both one and two different extraframework cation species) the mean Si-O-Si angles are larger than the corresponding Si-O-*X* angles. We have reported (Bell and Henderson, 2018) that this is the usual relationship for ordered $P2_1/c$ leucites and reflects the presence of weaker X-O bonds in the tetrahedral framework leading to greater degrees of framework collapse about the cavity cation sites.

The refined unit cell volumes for the X = Mg and X = Ni (see Table I) are approximately intermediate between the unit cell volumes for the corresponding structures with only one extraframework cation species. The unit cell volumes for the $Rb_2X^{2+}Si_5O_{12}$ structures are smaller than the volumes for the $RbCsX^{2+}Si_5O_{12}$ structures by approximately the same amount that the corresponding unit cell volumes are larger for

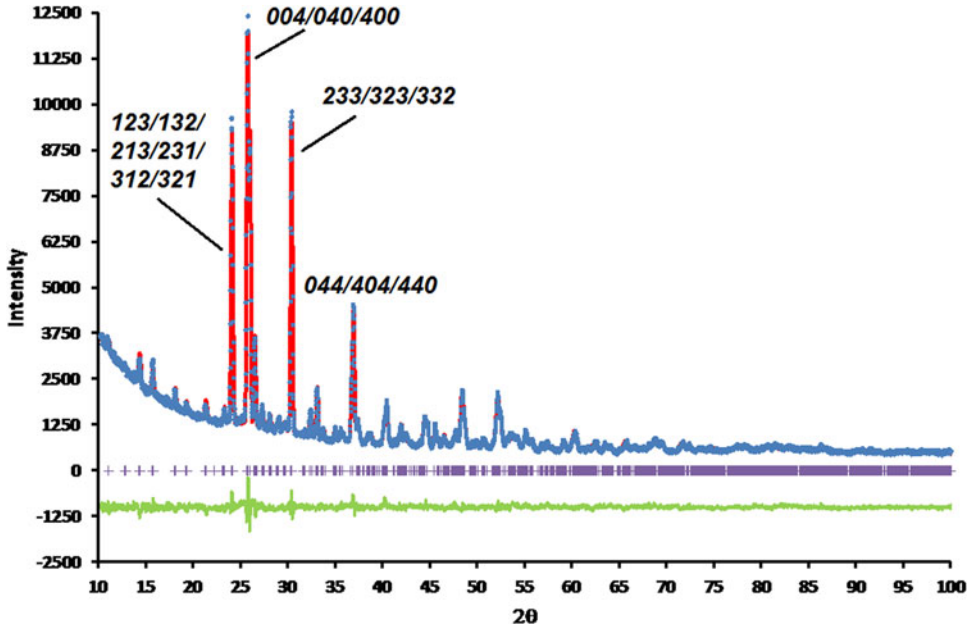

Figure 5. (color online) Rietveld difference plot for $RbCsCd^{2+}Si_5O_{12}$. Blue circles represent observed data points, red line represents calculated data points, green line represents difference curve and purple crosses represent positions of Bragg reflections. R-factors for this refinement were:- R_p = 3.5399, Rwp = 4.5294, R_{exp} = 3.0185, χ^2 = 2.2516. Miller indices are shown for some of the stronger peaks in the powder diffraction plot.

https://doi.org/10.1017/S0885715619000071 Published online by Cambridge University Press

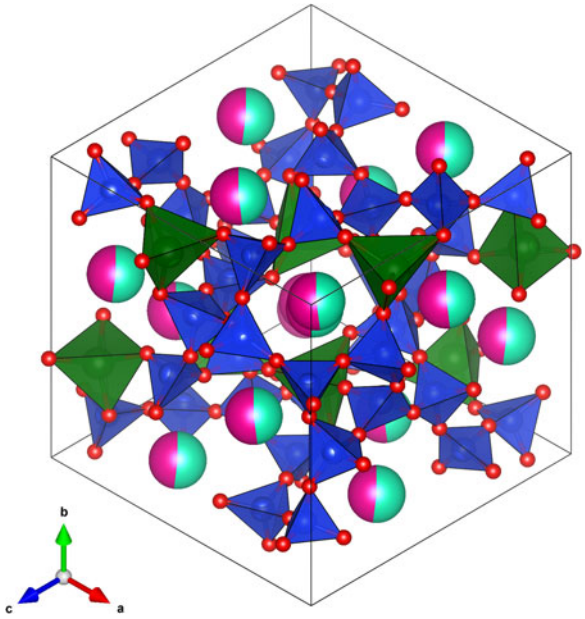

Figure 6. (color onlinr) VESTA structure plot for $RbCsCd^{2+}Si_5O_{12}$, viewed down [111] showing a channel for extraframework Rb^+ and Cs^+ cations. SiO_4 tetrahedra are shown in blue, CdO_4 tetrahedra are shown in green with O^{2-} anions are shown in red. Pink (Rb^+) and light blue (Cs^+) shadings show the occupancies of the two *A* cation sites.

$Cs_2X^{2+}Si_5O_{12}$ structures. However, for X = Cd (see Table I) the unit cell volume for the $Rb_2Cd^{2+}Si_5O_{12}$ structure is much smaller than that for the $RbCsCd^{2+}Si_5O_{12}$ structure, and the unit cell volume for the $RbCsCd^{2+}Si_5O_{12}$ structure is almost as large as the volume for the $Cs_2Cd^{2+}Si_5O_{12}$ structure. This relationship might suggest that the framework is close to being fully expanded for a mean cavity cation radius slightly lower than that for Cs.

IV. CONCLUSIONS

Crystal structures have been refined for $RbCsX^{2+}Si_5O_{12}$ (*X* = Mg, Ni, Cd) leucite analogues. These are isostructural with their *Pbca* $Rb_2XSi_5O_{12}$ and $Cs_2XSi_5O_{12}$ analogues. For *X* = Mg there is partial ordering of the Rb and Cs cations over the alkali metal cation *A* sites. However, for *X* = Ni and Cd these alkali metal cations are completely disordered.

SUPPLEMENTARY MATERIAL

The supplementary material for this article can be found at https://doi.org/10.1017/S0885715619000071.

ACKNOWLEDGEMENT

The authors wish to acknowledge the use of the EPSRC funded National Chemical Database Service hosted by the Royal Society of Chemistry.

Bell, A. M. T., and Henderson, C. M. B. (**1994a**). "Rietveld refinement of dry-synthesized $Rb_2ZnSi_5O_{12}$ leucite by synchrotron X-ray powder diffraction," Acta Crystallogr. **C50**, 984–986.

Bell, A. M. T., and Henderson, C. M. B. (**1994b**). "Rietveld refinement of the structures of dry-synthesized M Fe(III) Si_2O_6 leucites (M = K,Rb, Cs) by synchrotron X-ray powder diffraction," Acta Crystallogr. **C50**, 1531–1536.

Bell, A. M. T., and Henderson, C. M. B. (**1996**). "Rietveld refinement of the orthorhombic *Pbca* structures of $Rb_2CdSi_5O_{12}$, $Cs_2MnSi_5O_{12}$, $Cs_2CoSi_5O_{12}$ and $Cs_2NiSi_5O_{12}$ Leucites by Synchrotron X-ray powder diffraction," Acta Crystallogr. **C52**, 2132–2139.

Bell, A. M. T., and Henderson, C. M. B. (**2009**). "Crystal structures and cation ordering in $Cs_2MgSi_5O_{12}$, $Rb_2MgSi_5O_{12}$ and $Cs_2ZnSi_5O_{12}$ leucites," Acta Crystallogr. **B65**, 435–444.

Bell, A. M. T., and Henderson, C. M. B. (**2012**). "High-temperature synchrotron X-ray powder diffraction study of $Cs_2XSi_5O_{12}$ (*X* = Cd, Cu, Zn) leucites," Mineral. Mag. **76**(5), 1257–1280.

Bell, A. M. T., and Henderson, C. M. B. (**2016**). "Rietveld refinement of the crystal structures of $Rb_2XSi_5O_{12}$ (*X* = Ni, Mn)," Acta Crystallogr. **E72**, 249–252.

Bell, A. M. T., and Henderson, C. M. B. (**2018**). "Crystal structures of $K_2[XSi_5O_{12}]$ ($X = Fe^{2+}$, Co, Zn) and $Rb_2[XSi_5O_{12}]$ (*X* = Mn) leucites: comparison of monoclinic $P2_1/c$ and $Ia\bar{3}d$ polymorph structures and inverse relationship between tetrahedral cation (*T* = Si and *X*)—O bond distances and intertetrahedral *T*—o—*T* angles," Acta Crystallogr. **B74**, 274–286.

Bell, A. M. T., Henderson, C. M. B., Redfern, S. A. T., Cernik, R. J., Champness, P. E., Fitch, A. N., and Kohn, S. C. (**1994a**). "Structures of synthetic $K_2MgSi_5O_{12}$ leucites by integrated X-ray powder diffraction, electron diffraction and ^{29}Si MAS NMR methods," Acta Crystallogr. **B50**, 31–41.

Bell, A. M. T., Redfern, S. A. T., Henderson, C. M. B., and Kohn, S. C. (**1994b**). "Structural relations and tetrahedral ordering pattern of synthetic orthorhombic $Cs_2CdSi_5O_{12}$ leucite: a combined synchrotron X-ray powder diffraction and multinuclear MAS NMR study," Acta Crystallogr. **B50**, 560–566.

Bell, A. M. T., Knight, K. S., Henderson, C. M. B., and Fitch, A. N. (**2010**). "Revision of the structure of $Cs_2CuSi_5O_{12}$ leucite as orthorhombic *Pbca*," Acta Crystallogr. **B66**, 51–59.

Finger, L. W., Cox, D. E., and Jephcoat, A. P. (**1994**). "A correction for powder diffraction peak asymmetry due to axial divergence," J. Appl. Crystallogr. **27**, 892–900.

Gatta, G. D., Rotiroti, N., Fisch, M., Kadiyski, M., and Armbruster, T. (**2008**). "Stability at high-pressure, elastic behaviour and pressure-induced structural evolution of $CsAlSi_5O_{12}$, a potential host for nuclear waste," Phys. Chem. Minerals **35**, 521–533.

Momma, K., and Izumi, F. (**2011**). "VESTA 3 for three-dimensional visualization of crystal, volumetric and morphology data," J. Appl. Crystallogr. **44**, 1272–1276.

PANalytical (**2009**). *High Score Plus 2.2e (Computer Software)*. PANalytical, Almelo, The Netherlands.

Redfern, S. A. T., and Henderson, C. M. B. (**1996**). "Monoclinic-orthorhombic phase transition in the $K_2MgSi_5O_{12}$ leucite analog," Am. Mineral. **81**, 369–374.

Rietveld, H. M. (**1969**). "A profile refinement method for nuclear and magnetic structures," J. Appl. Crystallogr. **2**, 65–71.

Robinson, K., Gibbs, G. V., and Ribbe, P. H. (**1971**). "Quadratic elongation: a quantitative measure of distortion in coordination polyhedra," Science **172**, 567–570.

Rodríguez-Carvajal, J. (**1993**). "Recent advances in magnetic structure determination by neutron powder diffraction," Physica B **192**, 55–69.

van Laar, B., and Yelon, W. B. (**1984**). "The peak in neutron powder diffraction," J. Appl. Crystallogr. **17**, 47–54.